Ocean Engineering 266 (2022) 112717

Contents lists available at ScienceDirect

Ocean Engineering

journal homepage: www.elsevier.com/locate/oceaneng

Numerical modelling, manufacture and structural testing of a full-scale 1 MW tidal turbine blade

William Finnegan [a,b,*], Yadong Jiang [a,b], Patrick Meier [a,b], Le Chi Hung [a,b], Edward Fagan [a,b], Finlay Wallace [c], Conor Glennon [a,b,d], Michael Flanagan [a,b,d], Tomas Flanagan [d], Jamie Goggins [a,b,**]

[a] Civil Engineering, School of Engineering, National University of Ireland Galway, H91 HX31, Ireland
[b] MaREI Centre, Ryan Institute, National University of Ireland Galway, H91 HX31, Ireland
[c] Orbital Marine Power, Edinburgh, EH3 8BL, Scotland, United Kingdom
[d] ÉireComposites Teo, Inverin, Co. Galway, H91 Y923, Ireland

ARTICLE INFO

Keywords:
Composite materials
Manufacture
Numerical modelling
Structural testing
Tidal energy

ABSTRACT

Renewable energy is now accepted as the preferred alternative for electricity generation and as the replacement for fossil fuels. In recent years, tidal energy has shown promise as it is a more reliable source of renewable energy, compared to wind and solar, and 12 GWh of electricity from tidal energy was generated in 2020. As tidal technologies move closer to commercial viability, key components need to be optimised, tested and certified. Among the key components that need to be type-certified for tidal energy are the turbine blades.

In this study, a full-scale fibre-reinforced composite blade for use on 1 MW power generating nacelles of a tidal turbine was developed through numerical modelling, advanced manufacture technologies and state-of-the-art structural testing techniques. As a result of the high loads and harsh environment that a tidal turbine operates in, the blades have been manufactured using glass fibre reinforced powder epoxy and underwent an advanced structural testing programme that proved its structural integrity, where the results were used to validate the outputs from the numerical model of the blade. The load of 1,008 kN applied to the blade during the static testing was the highest load ever reported on a tidal turbine blade and this is the first time a large composite tidal blade has its equivalent design life of 20+ years through structural fatigue testing at full-scale.

1. Introduction

As the move from reliance on fossil fuels to renewable energy to power our daily lives picks up, tidal energy has emerged as a clean, reliable, predictable and dependable source of energy. By the end of 2020, 27.9 MW of tidal stream technology has been deployed in Europe since 2010. Of this, 10.1 MW is currently operating, where 17.8 MW has been decommissioned as projects have successfully completed their testing programmes (Collombet, 2021), which is almost four times as much as the rest of the world. The support for its development was boosted at the end of 2020 as the European commission published its EU Strategy on Offshore Renewable Energy, which sets a clear objective for ocean energy deployment of 100 MW by 2025 (EC, 2020).

Much of the technology for the key system components of a tidal energy converter can be sourced from the wind energy or marine sector. However, due to the high, concentrated loads imparted on the system, the tidal turbine blades – that convert the energy in the tidal current to useful mechanical energy that can be converted to electricity – need to be developed for this specific purpose. Additionally, the reliability of the blades is paramount to the success for the turbine. In order to aid in achieving this, the DNV GL standard, DNVGL–ST-0164 (DNV, 2015), provides details for the design, manufacture and testing of tidal blades. In recent years, there has been some success stories for the industry, including the Simec Atlantis Energy installation of a 1.5 MW bottom mounted tidal turbine installed in Scotland through the MeyGen project (SIMEC Atlantis Energy, 2022) and the installation of their AR500 tidal turbine in Naru Island, Japan (SIMEC Atlantis Energy, 2021), the Orbital Marine Power SR2000 floating tidal turbine achieving a world record delivery of over 3.2 GWh of tidal stream power to the UK grid (Orbital Marine Power, 2022), who have since grid-connected the next

* Corresponding author. Civil Engineering, School of Engineering, National University of Ireland Galway, H91 HX31, Ireland.
** Corresponding author. Civil Engineering, School of Engineering, National University of Ireland Galway, H91 HX31, Ireland.
E-mail addresses: william.finnegan@universityofgalway.ie (W. Finnegan), jamie.goggins@universityofgalway.ie (J. Goggins).

https://doi.org/10.1016/j.oceaneng.2022.112717
Received 9 December 2021; Received in revised form 19 August 2022; Accepted 23 September 2022
Available online 8 October 2022

generation of their device, the Orbital O2, and ORPC setting the US marine hydrokinetic turbine record with their deployment in Igiugig, Alaska (Garanovic, 2020).

The initial stage in the development of a tidal turbine blade is the design. Digital twins used for numerical modelling offer an efficient alternative to physical testing in order to develop and test initial design concepts. Learning from the wind energy sector, modelling methodologies that use layered shell elements have been employed in the design of tidal turbine blades (Fagan et al., 2016; Finnegan et al., 2020; Jiang et al., 2019; Murray et al., 2016). Building on these, Finnegan et al. (2021a) compared the use of a number of commercial finite element software packages that used this methodology and validated the results against the experimental testing of a composite turbine blade.

As the tidal energy sector develops, fibre-reinforced composite materials, similar to wind, are being used for the manufacture of tidal turbine blades. However, due to the high loadings during operation, thick section composite is required for key structural parts of the blade. Vaidya et al. (2001) presented the processes required for the production of thick-section composite parts using cost-effective liquid moulding processes, such as resin transfer moulding and vacuum assisted resin transfer/infusion moulding. Maguire et al. (2018) described the manufacturing process in detail as they characterised epoxy powders for processing thick section composite structures, including a description of the relationship between glass transition temperature and the degree-of-cure. Additionally, Maguire et al. (2017) used finite element software to model the resin transfer during the manufacturing thick section parts with low-cost fibre reinforced polymers, and Matveev et al. (2019) performed a numerical study to investigate the required processing conditions of thick section composite structures, in order to analyse their effect on consolidation of thick composite components.

Prior to deploying tidal turbine blades, it is essential that a structural testing campaign is performed to ensure that the blades have the required structural integrity. Along with the DNV GL standard (DNV, 2015), there is also an IEC test specification, IEC 62600–3:2020 (International Electrotechnical Commission (IEC), 2020), for structural testing of tidal turbine blades. As the results from these testing campaigns are often commercially sensitive, only a limited amount of publications relating to large-scale tidal turbine blade tests exist. The results from the fatigue testing of a 3/8th scale blade and rotor subsection for the OpenHydro prototype tidal turbine that was exposed to approximately 1,000,000 fatigue cycles is presented in de la Torre et al. (de la Torre et al., 2018). Recently, Meier et al. (2020) completed a static and fatigue testing programme on a full-scale helical foil for the ORPC device, which was subsequently deployed for operation in Alaska, USA, and Glennon et al. (2021) detailed the fatigue testing programme on a full-scale prototype blade developed by Schottel Hydro for Sustainable Marine's novel floating tidal energy system, where the blade underwent fatigue loading that was equivalent to 20 years of operation.

In this paper, a full-scale fibre-reinforced composite blade for use on 1 MW power generating nacelles of a tidal turbine is developed from design to structural testing. The tidal turbine blade is manufactured using glass fibre reinforced powder epoxy and designed using a digital twin in the form of a numerical finite element model, which is validated using the results from the structural testing in this paper. Due to the high loads and harsh environment that a tidal turbine operates in, advanced manufacturing technologies have been developed to produce thick section composites in excess of 130 mm for the key structural elements (i.e. the spar caps and at the root). The blade is manufactured in a single cure "one-shot" process which allows continuous fibres to be laid up across all bond lines and facilitates the inclusion of high-friction root insert connections in a single process without the need for adhesives. The full-scale tidal turbine blade then undergoes an advanced structural testing programme that proves its structural integrity, where it is the largest blade to undergo a full lifetime fatigue programme (equivalent of 20+ years) and has the highest load ever reported on a tidal turbine blade. This adds significantly to the current state-of-the-art for the manufacture and testing of composite tidal turbine blades.

2. Materials and methods

2.1. Aim and objectives

The overall aim of this study is to develop the next generation of robust composite tidal turbine blades using advanced composite technologies. This is achieved through the development of a full-scale fibre-reinforced composite blade for use on 1 MW power generating nacelles of a tidal turbine, which is broken down into three main stages – design, manufacture and testing. Therefore, in order to achieve the aim of the study, a number of objectives must be achieved:

- To develop a numerical finite element (FE) analysis model to aid in the design of the composite tidal turbine blade.
- To manufacture a full-scale blade using advanced composite manufacturing technologies.
- To validate the performance of the design and manufacturing process through static and fatigue testing of the full-scale blade.

2.2. Methodology

In this paper, the development of the full-scale fibre-reinforced composite blade for use on 1 MW power generating nacelles of a tidal turbine is broken down into three main stages – design, manufacture and testing, where their interaction is illustrated in Fig. 1. The design aspect that is explored is the numerical simulation of the composite layup of the blade using a FE model, which was developed using BladeComp (Jiang et al., 2021a). The composite tidal blade has been manufactured using a range of advanced composite manufacturing technologies, which are based on the advanced glass fibre reinforced powder epoxy composite material. The blade then underwent a comprehensive structural testing programme, which included static, dynamic and fatigue tests, to ensure it had the structural integrity to withstand operational and maximum loadings over its design life of 20+ years. The results of this testing programme were then used to validate the numerical FE model used in the blade design. Further details on the main stages of the development are presented in the remainder of Section 2, where the results from the testing programme, along with the FE model validation, are presented in Section 3, followed by discussions and conclusions.

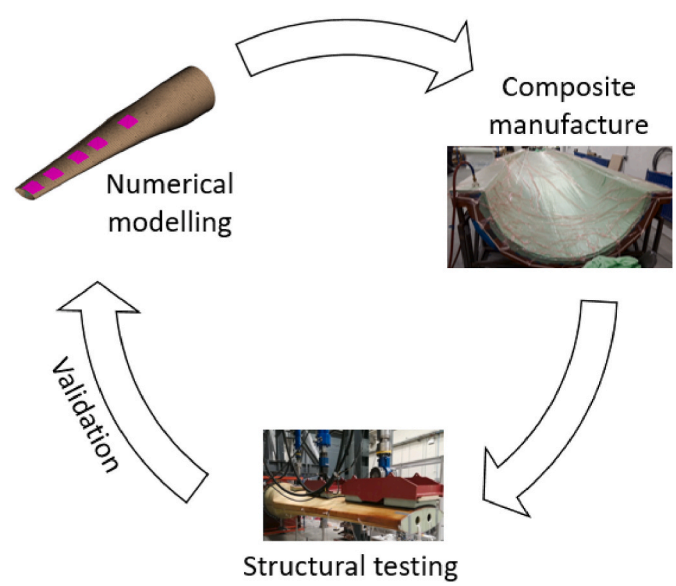

Fig. 1. Methodology for developing and testing a full-scale tidal turbine blade that is used in this study.

2.3. Turbine and blade description

The blade presented in this paper is part of the development of Orbital Marine Power's O2 turbine, which has two 1 MW 2-bladed turbine of 20 m rotor diameter, resulting in a 2 MW device. The O2 tidal turbine has been deployed in the Fall of Warness at the European Marine Energy Centre (EMEC) in 2021, where tidal speeds can exceed 3 m/s. It has been connected to the local electricity grid and will help power the communities of Orkney cleanly and sustainably from the waters that flow past their islands. The previous generation of this device achieved a world record delivery of over 3.2 GWh of tidal stream power to the UK grid. For the purpose of this study, the main structural elements of the blade were manufactured and tested, meaning that the hydrodynamic fairing along the trailing edge and at the tip were not included in the study. Therefore, the overall length of the test blade is approximately 8 m, where the blade is shown in Fig. 2. The final mass of blade is 4,485 kg, where the centre of gravity is located at approximately 2.5 m form the blade root.

2.4. Numerical modelling

2.4.1. Geometry and structure

Besides the physical testing, a finite-element (FE) model of the tidal turbine blade is developed and validated against the testing data. Since this tidal turbine blade was manufactured using the same technique as the wind turbine blades, the blade can be considered to be a thin-body structure. Hence, the shell element SHELL281, which contains 8 nodes with six degrees of freedom at each node, is selected to construct the blade FE model. Layered shell sections with multiple plies (3 integration points per ply) are assigned to each shell element according to the blade structure details. Since the blade external surface is used to generate the shell elements, the plies on of each element are configured to stack from the element plane towards the blade inner space. Similar to the blade external surface, the web is constructed using shell elements SHELL281. However, these elements are meshed along the middle plane of the web and their plies are configured to stack symmetrically about the element plane. Considering the complexity of the structural details, the FE model of the tidal turbine blade was generated in software Ansys® Academic Research Mechanical, Release 17.1 (ANSYS, 2016) using the in-house BladeComp software (Jiang et al., 2021a), where further details of the model are available at (Jiang et al., 2021b). Fig. 3 shows the meshed FE model generated for simulating the static tests.

Fig. 2. The tidal turbine blade being unloaded for structural testing (without the blade tip and trailing edge fairings).

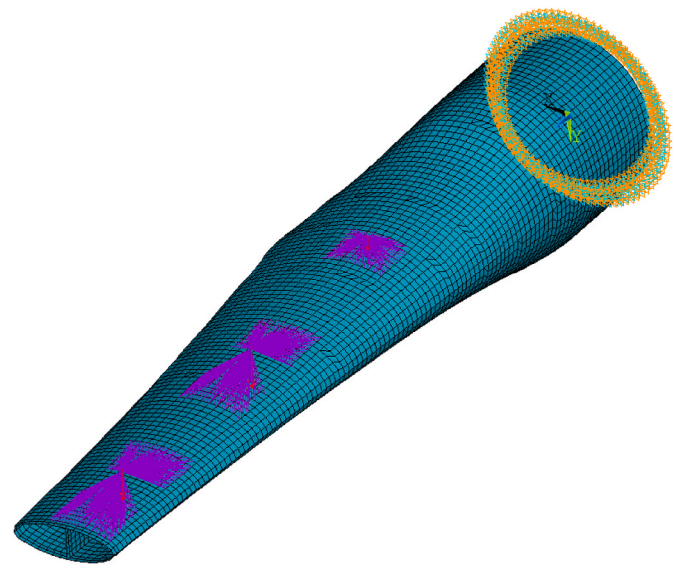

Fig. 3. FE model generated in Ansys® Academic Research Mechanical, Release 17.1 (ANSYS, 2017).

2.4.2. Boundary conditions

For simplifying the model, the connections between the upper half, lower half and the web are assumed to be strong enough to resist the loads imparted. Hence, the bonding details are neglected and the blade is modelled as an integrated part, which is a reasonable assumption as the connections are manufactured using a one-shot process, with continuous fibres running across the bond lines rather than adhesives. Similarly, the steel support frame is considered to hold the blade efficiently, which is in line with the test observations. Hence, it is not included in the FE analysis, and instead, the displacements of the nodes on the blade root section are constrained. To simulate the load introduction mechanism, the mesh nodes which were supposed to be in contact with the load transfer pads were selected The point loads applied from the three actuators are distributed to the selected nodes through multipoint constraint elements (MPC184) as shown in Fig. 3. In total, the FE model contains 11615 nodes, 3898 SHELL281 elements and 564 MPC184 elements.

Static analyses are performed to validate the accuracy of the developed FE model as the tests are considered to be quasi-static. The strain and deflection values predicted from the analyses are compared with the data recorded by the strain gauges and the displacement transducers, which are detailed in section 3.

2.5. Blade manufacture

The tidal turbine blade developed in this paper was manufactured at ÉireComposites in Galway (Ireland) from a glass fibre reinforced powder epoxy composite material using a number of advanced manufacturing technologies. Many of these technologies were developed during this programme of research, which also included a series of coupon and demonstrator trials, where further details are available at (Finnegan et al., 2021b). These advanced manufacturing technologies are summarised as follows:

- Glass fibre reinforced powder epoxy composite material.
- Thick section laminate manufacturing, which is vital at the key structural elements, in particular in the spar caps and at the root.
- Robust root connection, where novel high-friction root inserts were used.
- One-shot manufacturing process with continuous fibres running across the bond line, which have greater strength than adhesive

bonds at joints and reduces stiffness inconsistences at bond lines (for example, along the leading and trailing edge of the blade).

The main novelty in the manufacturing process comes with the challenges that are overcome due to the size of the blade, resulting in thickness composite sections (>130 mm in places), the fast changes in geometry over a short length and the required durability of the material in the marine environment. The remainder of this section outlines the manufacture of the full-scale fibre-reinforced composite tidal turbine blade.

2.5.1. Blade materials

The primary material that is used to manufacture the tidal turbine blade in this study is glass fibre reinforced powder epoxy composite material, which is based on ÉireComposites' Composites Powder Epoxy Technology (CPET). CPET has been presented previously in (Maguire et al., 2018, 2020; Brádaigh et al., 2013) and has a number of advantages over traditional composite materials, including small through-thickness wet out requirement, good fibre volume fraction control at material manufacture stage, low exothermic during cure and it requires a vacuum bag only, out-of-autoclave cure. Additionally, the raw material can be stored at ambient temperatures and has a very long shelf life, when compared to tradition epoxy resins. Prior to the manufacture of the full-scale tidal turbine blade, an experimental investigation of coupons, manufactured from glass fibre reinforced powder epoxy composite material, was performed. This explored the effect of water ingress on the material properties, which was accounted for in the blade design, building on the previous work of (Grogan et al., 2018) and (Michael et al., 2019). Unidirectional glass fibre reinforced CPET is used in the manufacture of the main structural elements of the tidal turbine blade, which are the spar caps and web. The main blade structure consists of an upper and lower blade half connected at the leading and trailing edges with a single internal shear web. The blade trailing edge fairings and the blade tip are constructed separately to the main body of the blade and adhesively bonded to the finished structure. These two components do not resist the primary hydrodynamic loads, instead they maintain the optimum hydrodynamic shape of the blade; hence, they are not considered in the full-scale structural tests. The root of the blade connects to the turbine pitch bearing via 48 steel root inserts. The root connections are made from S355 grade steel, which is a medium tensile, low carbon manganese steel. These are embedded into the root of the tidal turbine blade during the composite material lay-up and bonded within the blade during the curing. The inserts contain M36 female threads and are equally spaced on a pitch circle diameter of 1400 mm.

2.5.2. Blade manufacturing process

Unlike traditional glass fibre epoxy manufacture, where exotherm from the resin during cure must be controlled to avoid damage to the part or a potential health and safety hazard (Gurit, 2016), there is no significant exotherm during the one-shot manufacturing process for CPET. The one-shot manufacturing process for CPET was introduced in (Brádaigh et al., 2013; Flanagan et al., 2015) and the details for how it has been applied for the manufacture of a large tidal blade are given in this section.

The material is solid at room temperature but is formable, without polymerisation, at low temperatures. This means that individual substructure components can be formed off-line on low cost, low temperature tooling and assembled to form the final part, which is then polymerised during the one-shot cure. A distinct advantage is this process enables the manufacture of large parts with complex internal structures without secondary bonding procedures. Therefore, eliminating the need for gluing along the bond line, which is further reinforced by continuous fibres, resulting in a stronger bond when compared to traditional manufacturing techniques, which is evident from the results from the lap shear testing presented in Finnegan et al. (2021b). Additionally, it enables joints with complex ply drop-offs and overlaps that would be difficult or impossible with traditional bonding techniques. CPET forms a bond to metal during cure which allows metal inserts to be embedded in the layup during cure, eliminating the need to drill and glue inserts. Furthermore, there are no volatile organic compounds emitted during cure, which means that the manufacturing process is in line with the tightest European manufacturing regulations (VOC, 1999). The material is supplied in a semi-pre-impregnated form, where the glass is uniformly coated in powder epoxy. This means that during cure the powder epoxy only has to travel through the thickness of one ply in order to ensure that the laminates are fully wet-out and that there is uniform fibre volume throughout the entire structure.

Therefore, this blade manufacturing process has a number of advantages over traditional blade manufacturing that have developed in the wind energy sector for many years. However, there are some drawbacks that need to be overcome to make the process more efficient when moving to commercial production is improving the installation method for the metal inserts as it can be a slow, laborious process and the extra b-stage cures that are required, but the cure timings could be optimised during large volume production to reduce energy usage. In addition, this process is only suitable for manufacture of blades that are short enough to fit in a large industrial oven, which may be limitation for some composite manufacturers.

An overview of the main manufacturing processes involved when using the one-shot CPET process to produce a tidal turbine blade are shown in Fig. 4, which are as follows:

1. Moulds are manufactured for the tidal turbine blade components from a high-temperature epoxy reinforced with glass fibre composite material, which is cured and finished. This mould has been designed and manufactured so that it can withstand repeated heating and cooling cycles, making it suitable for volume production.
2. Plies of the glass fibre reinforced CPET are laid up on the mould, which has been derived from the design, based on the numerical model developed in Section 2.4. When the root section is being laid up, the steel root inserts are installed so that they are co-cured with the blade to ensure a rigid bond between the steel and composite.
3. At several stages during the layup of thick sections the layup is vacuum bagged and a 50 °C cure, referred to as a b-stage cure, is carried out in order to minimise voids. After the b-stage cure is carried out the layup is, de-bulked and consolidated but it is not cured.
4. Once the layup of a sub component is complete, the blade component is vacuum bagged and a final b-stage cure is carried out. This b-stage cure results in a consolidated solid sub-component which can then be assembled to form the final blade.
5. The blade web is manufactured separately and then installed between the upper and lower blade sections. To ensure the web is bonded rigidly in place during the final cure, composite L-brackets are installed on the upper and lower blade sections. These L-brackets ensure that there are co-cured continuous fibres running across all bond lines.
6. The main components (i.e. the upper and lower blade sections and the web) are then assembled. Having each sub-component b-stage cured means that these components are solid, un-cured laminates, which can easily be handled and machined prior to assembly. This allows for complex geometries with continuous fibres across the bond line to be assembled.
7. This final assembly is then vacuum bagged in place for the final one-shot cure at 180 °C.
8. Once the cure cycle is complete, the moulds and vacuum bag are removed, resulting in the final one-shot tidal turbine blade, without any structural adhesives, which is ready for testing. If the blade was, instead, going to be installed on tidal turbine for operation, hydrodynamic faired components (along the trailing edge and blade tip) would be installed, along with the blade central void being filled with foam and outer blade finishes applied.

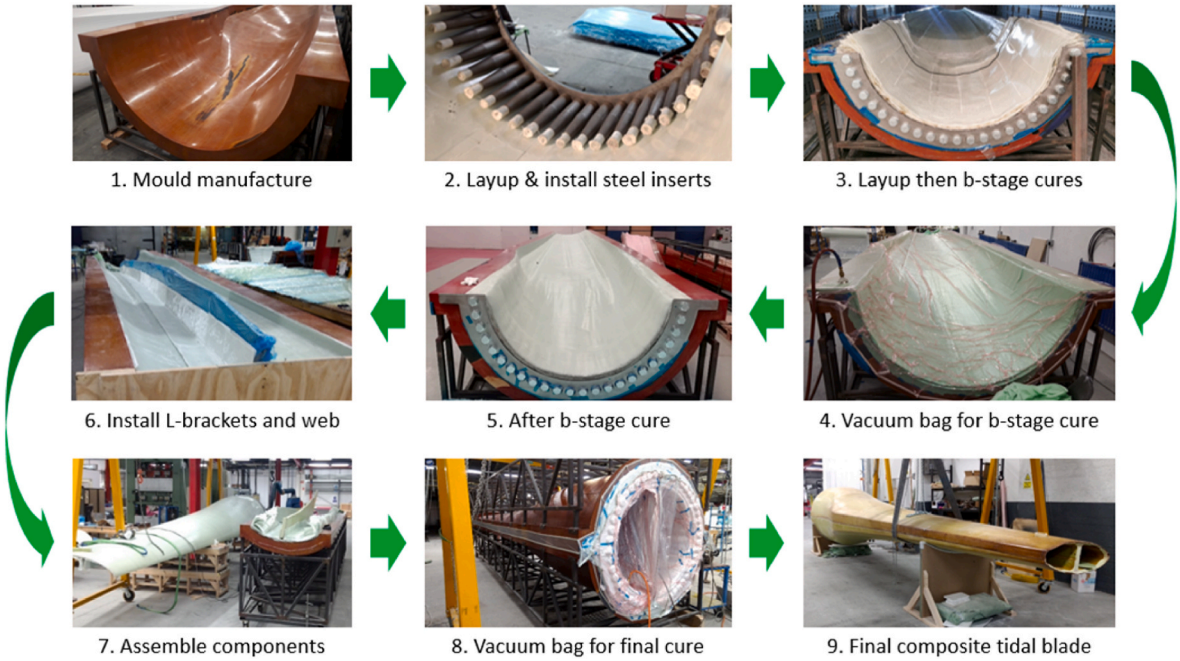

Fig. 4. Summary of the manufacturing stages required for the composite tidal turbine blade.

2.6. Structural testing

Once the tidal turbine blade was manufactured, it was transported to the Large Structures Testing Laboratory in the National University of Ireland Galway (NUI Galway) to undergo a comprehensive structural testing programme.

2.6.1. Test setup

The tidal turbine blade was supported at its root on the support frame. The support frame was constructed from a steel cylinder providing adequate stiffness and load transferral to 9 bolts on the strong floor (3 bolts at the root of the blade and 6 bolts at the other end). An overview of the test setup is shown in Fig. 5.

The blade was loaded via three hydraulic actuators ranging in capacity from 240 kN to 750 kN, which are shown in Fig. 5. The actuators hung from the modular steel frame and applied loads vertically only. The three actuators can be controlled separately and in unison for application of complex loading patterns for static and fatigue testing. The load was applied to the surface of the blade through five contact pads and three load introduction mechanisms. The mechanisms split the load from each actuator to two contact pads for the two larger actuators, thereby increasing the number of loading points to 5 (from 3 actuators) and increasing the accuracy of the applied bending moment and shear force profiles along the blade in line with the design loads.

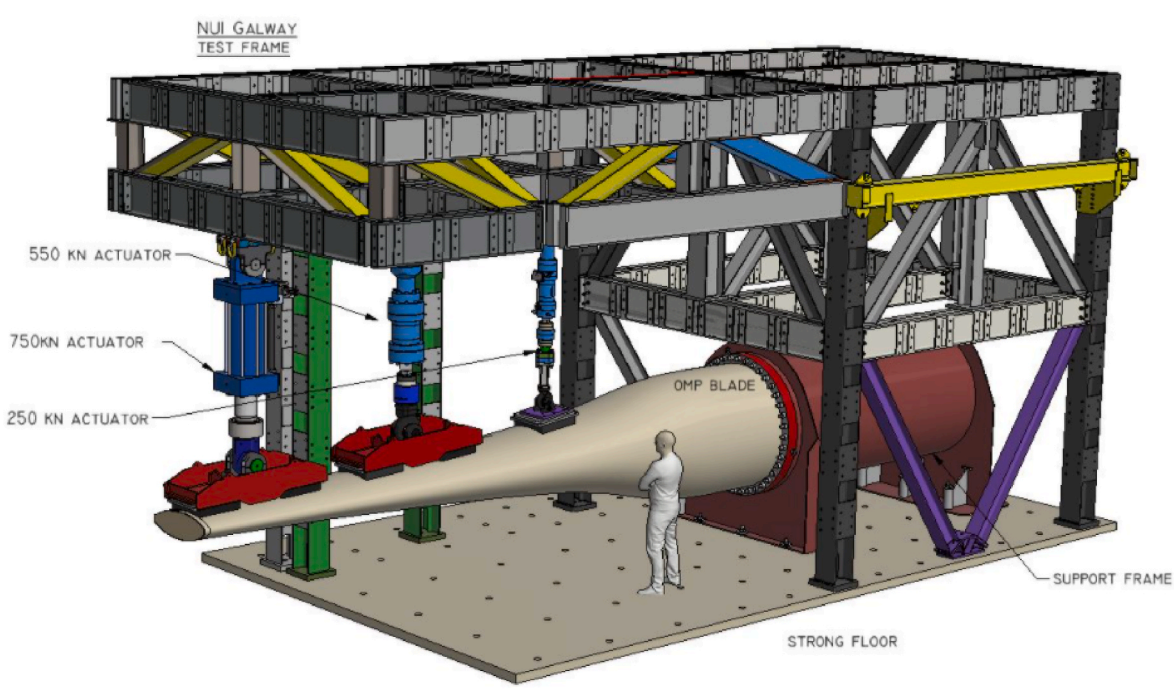

Fig. 5. 3D rendering of the test setup with the major components highlighted. Note: Some support columns have been removed from the rendering for clarity.

2.6.2. Data acquisition and instrumentation

During the testing programme, the performance of the tidal turbine blade test specimen was monitored using a range of instrumentation, where their output was recorded using a Labview program for the duration of the test. The instrumentation used during testing includes:

- Electrical resistance strain gauges (6 mm) were applied to the surface of the blade (both linear and rosette gauges were used), with a strain limit of 3% (30000×10^{-6} strain). The strain gauges have a fatigue life of 1×10^{6} at $\pm 1500 \times 10^{-6}$ strain and are, therefore, suitable for the fatigue tests in this study. The strain gauges were manufactured by Tokyo Measuring Instruments Laboratory Co., Ltd., where the linear gauges were model FLA-6-11-3LT and the rosette gauges were model FRA-6-11-3LT.
- Two types of displacement transducers – string pot displacement sensors, with a range of up to 500 mm (micro epsilon WDS-500-P60-CR-P), and linear variable differential transformers (LVDTs), with a range of ±5 mm for the LVDTs at the root (RDP D6/05000A) and a range of ±25 mm for the LVDTs along the length of the blade (RDP ACT1000A).
- Videometric measurements using a 3D laser scanner (Leica Scan-Station C10) and a digital image correlation (DIC) system (GOM ARAMIS).
- Load cells at each hydraulic actuator, which were manufactured by Zwick Roell.

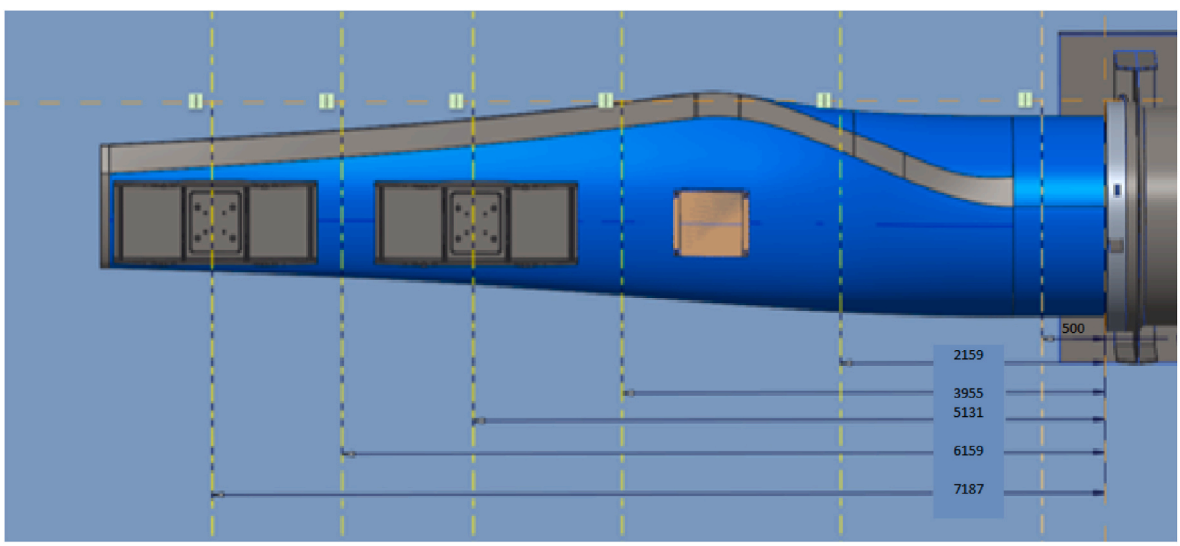

(a)

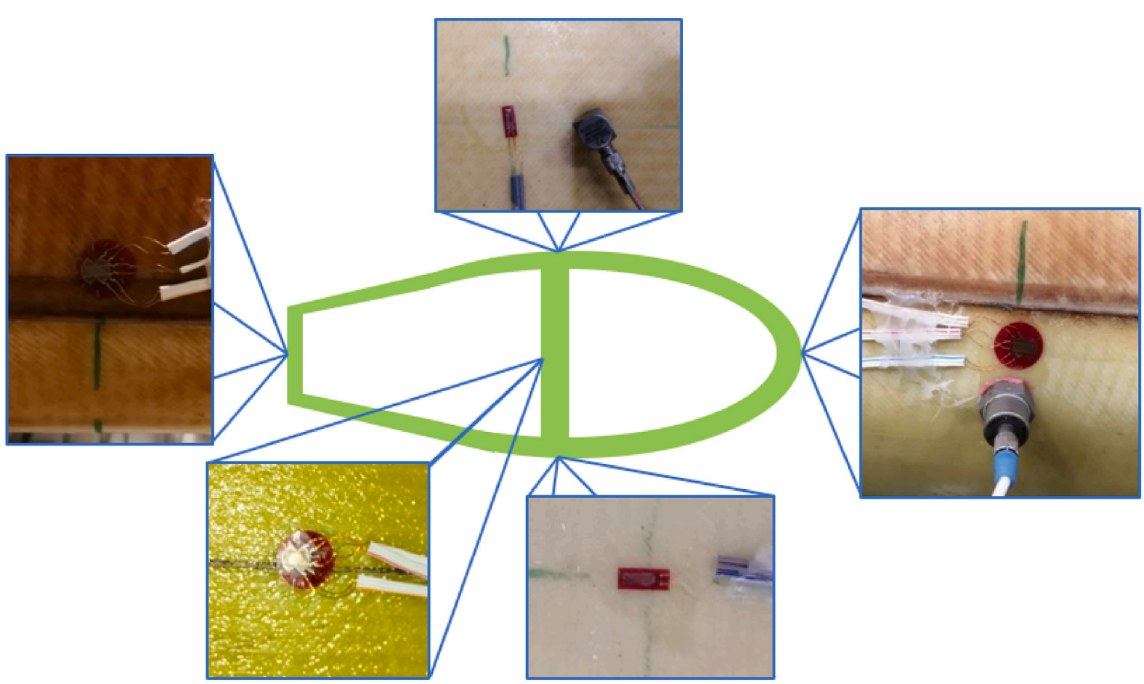

(b)

Fig. 6. Schematic of the locations of the sensors on the tidal blade, where (a) is the distance of the 6 cross-section planes along the blade with instrumentation from the blade root and (b) is the typical instrumentation at each cross-section, including linear and rosette electrical resistance strain gauges and accelerometers.

- Accelerometers for the dynamic (natural frequency) tests, which have a range of 1–8000 Hz.

Instrumentation along the blade was placed at 6 cross-section planes along the blade (as shown in Fig. 6 (a)). The layout of the sensors at each of these cross-section planes was very similar, where a typical instrumentation along the cross-section is shown in Fig. 6 (b).

In total, the tidal turbine blade was monitored using 12 linear strain gauges, 18 rosette strain gauges, 7 displacement sensors, 7 accelerometers and 3 load cells to capture its response during the structural testing programme. The outputs from these sensors have been processed and analysed, where selected results are presented in Section 3.

2.6.3. Testing programme

The blade was installed at 6° (to the chord line of the blade at the tip), which can be seen in Fig. 7, and a single design load profile was used, which incorporated both flapwise and edgewise loads. The load profile was derived from the operational loading observed by the developer for the previous version of the tidal turbine in accordance to the methodology in the DNVGL-ST-0164 standard (DNV, 2015). The testing programme was performed in line with the DNVGL-ST-0164 standard and the IEC 62600–3:2020 testing specifications (International Electrotechnical Commission (IEC), 2020). As per the aforementioned standards, several partial load factors were applied to the maximum design loads to account for uncertainties in construction materials, load and test scatter when performing full-scale testing. The temperature in the laboratory was maintained at approximately 19 °C for the duration of the testing programme and was monitored throughout the testing programme. Torsional extreme loads were not considered to be critical for the blade design. The fatigue testing programme for the blade included:

- Dynamic testing – to determine the natural frequencies and associated damping of the blade.

Fig. 7. The full-scale tidal turbine blade installed for structural testing.

- Initial static testing (at 100% design load case) – the design load was applied to the tidal turbine blade in increments of 12.5% up to a maximum design load (100%), where the total force applied to the blade between the 3 actuators was 1008 kN.
- Fatigue testing – this was divided into two testing phases. Phase 1 used the actual load, which was determined from previous operational trials, accelerated for the laboratory testing and cycled for 200,000 cycles, which is the equivalent of 20-years operation at the actual load. Phase 2 used the load was factored by 1.39, to allow for factors of safety, and cycled for 100,000 cycles, which is the equivalent of 20-years operation at the factored load.
- Residual strength testing, which includes both static (at 100% design load case) and natural frequency tests after each fatigue test has concluded.

3. Results

This section primarily looks at the results from the structural testing of the blade, as it is the culmination of the research, along with the validation of the numerical model against the static testing results. Therefore, this section is structured in line with the testing programme outlined in Section 2.6.3.

3.1. Dynamic testing

Dynamic testing was performed in order to determine the natural frequencies and associated damping of the tidal turbine blade. In order to monitor this, accelerometers were installed on the blade, where:

- 8 single-axis accelerometers were installed on the pressure side of the blade to estimate the flapwise natural frequencies
- 3 single-axis accelerometers were installed on the leading edge of the blade to estimate the edgewise natural frequencies
- 1 additional single-axis accelerometer was installed on the pressure side of the blade to estimate the torsional natural frequency

Using these accelerometers installed on the blade to record the response, the tip of the blade was hit in the flapwise direction with a hammer to excite it, which was repeated 3 times, and then hit in the edgewise direction (and repeated 3 times). For each recorded acceleration data, modal analysis, based on the Fast Fourier transform (FFT) algorithm, was carried out to obtain the response spectra at different blade locations. According to the magnitudes and phases given by the FFT analysis, the blade natural frequencies in different vibration directions were figured out. In this study, the first two natural frequencies in the flapwise direction, the first two natural frequencies in the edgewise direction and the first torsional natural frequency are of interest, as suggested in IEC 62600–3:2020 standard (International Electrotechnical Commission (IEC), 2020). The half-power bandwidth method (Chopra, 2007) was selected for calculating the damping ratios of the five vibrating modes. The average results obtained from different accelerometer locations were taken as the natural frequencies and damping ratios of the blade. Three dynamic tests were performed under each impact direction and the average results were used to estimate the natural frequencies, natural period and damping ratios of the blade, which are summarised in Table 1.

Table 1
Natural frequencies and associated damping of the blade.

Mode #	Frequency [Hz]	Period [s]	Damping (%)
1st Flapwise	15.3	0.07	0.40
1st Edgewise	17.8	0.06	0.35
2nd Flapwise	31.3	0.03	12.64
2nd Edgewise	31.5	0.03	2.23
1st Torsional	84.5	0.01	0.30

3.2. Static testing

Static testing of the tidal turbine blade is performed to determine the structural strength of the blade. Therefore, it includes applying the maximum design static load to the blade in order to demonstrate the blade can withstand this load, which includes for partial load factors to account for uncertainties as per IEC 62600–3:2020. The load was applied in increments of 12.5% up to the maximum design static load (100%) through the 5 contact pads (with centres at 3.28m, 4.63m, 5.63m, 6.69m and 7.69m from the root) using the multi-actuator load introduction system. The load was held for a duration of 30 s before being relaxed and the loading were repeated at least 3 times to ensure repetition. The resulting normalised blade deflections are shown in Fig. 8 for each of the 8 load cases (12.5%, 25%, 37.5%, 50%, 62.5%, 75%, 87.5% and 100%), where these have been normalised against the highest tip deflection (at the 100% static test load case) of 109 mm. This is the deflection of the blade only as it has been corrected to allow for movement in the root support frame, which was monitored with LVDTs during the testing programme. At a tip deflection of 109 mm, there was a torsional twist of 0.17° at the tip towards the leading edge.

The resulting strains along the outer surface of the blade in the middle of the spar caps (on the pressure (top) and suction (bottom) side of the blade) have been normalised against the highest strain monitored and are shown in Fig. 9. The highest strain monitored on the pressure side of the blade is 0.001974 (positive sign indicates the material is in tension) and the highest strain monitored on the suction side of the blade is −0.001969 (negative sign indicates the material is in compression), which both occurred 3.96m from the blade root. These highest compression and tension strains can be seen in Fig. 9 (a) and Fig. 9 (b), respectively. The blade substrate is glass fibre reinforced powder epoxy, where no failure in the material is expected until strains well in excess of ±0.0025 occur. Therefore, the blade design and manufacturing processes used are adequate to withstand the maximum design static loads.

3.2.1. Comparison to numerical model

The digital twin, in the form of a numerical FE model that is presented in detail in (Jiang et al., 2021b), which was used to design the blade could be validated by comparing its predictions with the results from the structural testing programme. Therefore, the deflections predicted by the numerical FE model have been compared to the test data in Table 2, where the two sets of data are in very good agreement, as a difference of less than 8.5% was observed (see Table 2). The strain along the surface of the blade has also been predicted by the numerical FE model and has been compared to the strain sensor data recorded during the static testing programme. The comparison of the maximum tensile strain at the outer surface at the top spar cap and the compressive tensile strain at the outer surface at the bottom spar cap is shown in Table 2 for 4 of the load cases, where the maximum strains predicted by the numerical FE model are in good agreement with those observed during the static testing programme, as a difference of less than 8% in tension and less than 17.1% in compression was observed (see Table 2). Therefore, the accuracy of the numerical FE model that was used as a digital twin to design the blade has been validated.

3.2.2. Static testing of the load-application duration

The loads used to derive the maximum static load only occur on the blades for a very short duration. Therefore, in order to be conservative and avoid shock-loading the blade, the static test load was held for a duration of 30 s, which is in line with that specified in the DNVGL-ST-0164 standard of at least 10 s.

However, the IEC DTS 62600–3 testing specifications state that "for TECs the recommended minimum duration of the test load is 6 h, about equivalent to half of a single tidal cycle in a diurnal tidal pattern". Therefore, a 6-h (21,600 s) static test at the 100% load case was performed on the blade to investigate if it was necessary for the blade and setup used in this study.

The variation of the load on the blade and the deflection of the blade during the 6-h static test are presented in Fig. 10. It is evident from this figure is there was no significant change of the overall system during the 21,600 s. However, after approximately 12,000 s, there is a slight shift in the loading due to a slight slip of the middle contact pads towards the tip. However, this had no significant impact on the test. This shows that

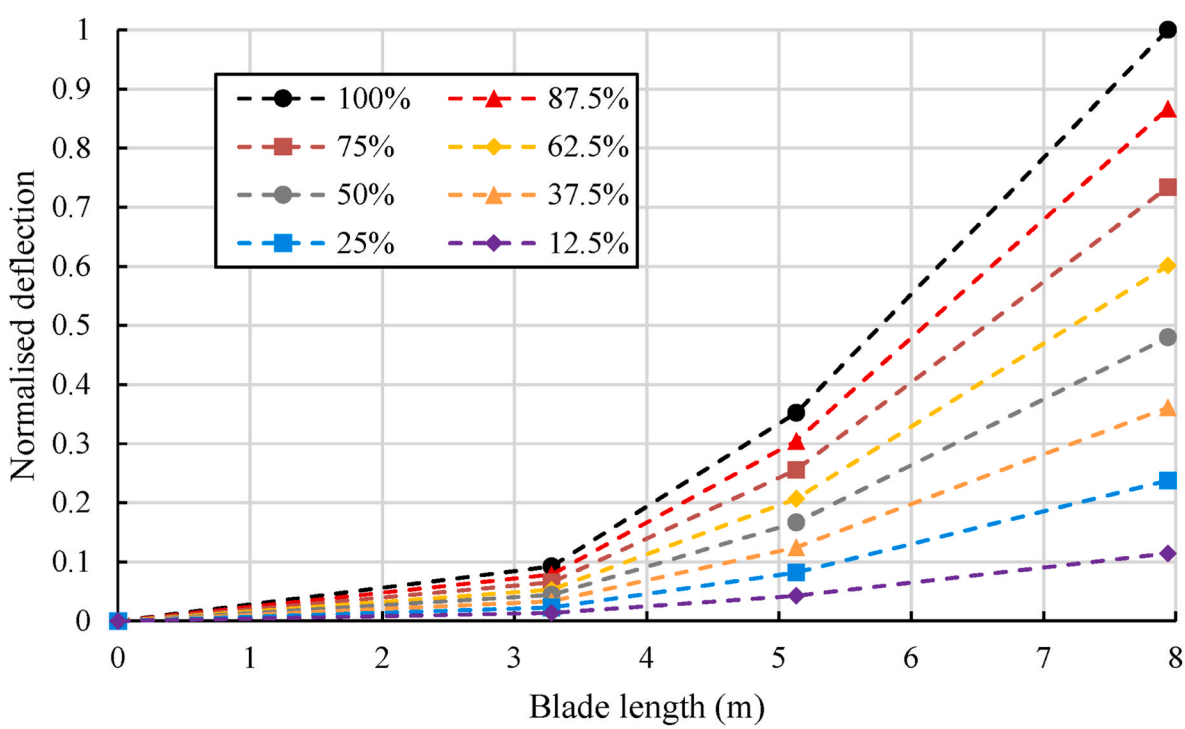

Fig. 8. Normalised deflection of the blade observed during the physical testing along the length of the blade
Note: normalised deflection to the tip deflection at the 100% load case.

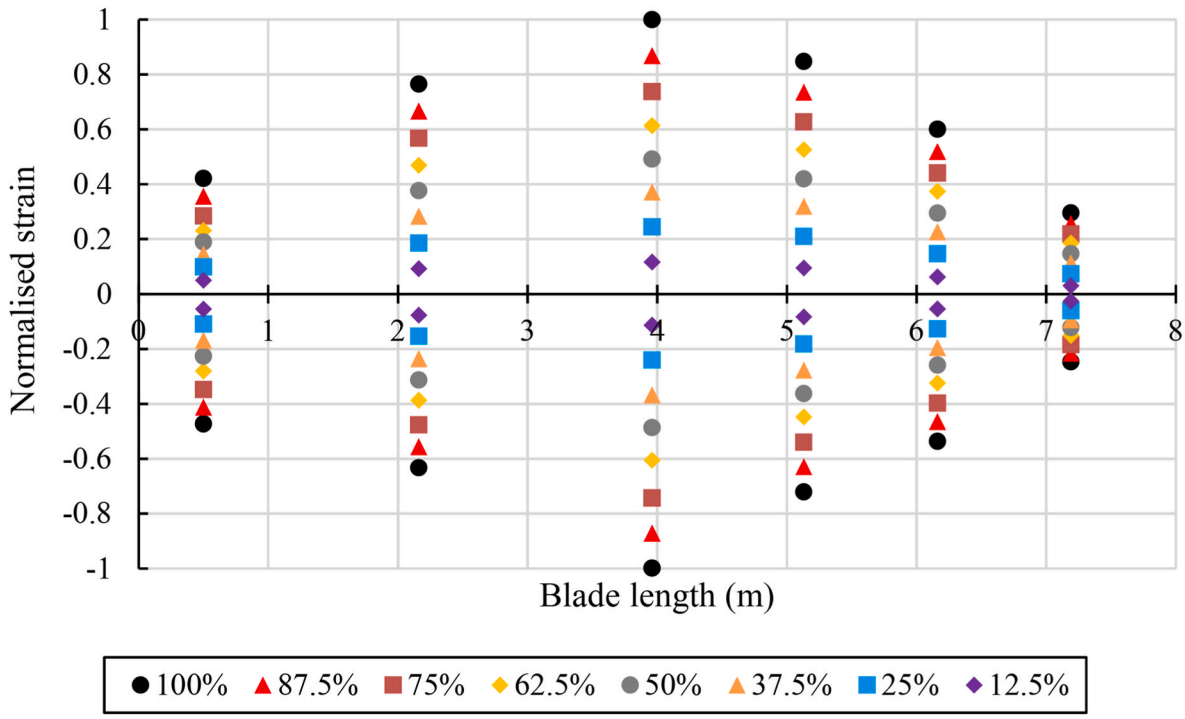

Fig. 9. Normalised strain recorded during the static testing along the length of the blade, where positive strain values occur at the outer surface at the top spar cap, which is in tension, and negative strain values occur at the outer surface at the bottom spar cap, which is in compression. Note: normalised strain to the 100% load case.

Table 2
Comparison between the tip deflection, maximum tensile/compressive strains observed during the experimental testing and outputs form the numerical model (Jiang et al., 2021b), where the maximum strains observed occurred at 3.96m from the blade root.

	Static load case			
	25%	50%	75%	100%
Tip deflection (mm)				
Experimental testing	26	52	80	109
Numerical model	24.9	49.8	74.6	99.7
Difference	−4.2%	−4.2%	−6.8%	−8.5%
Maximum tensile strain ($x10^{-6}$) recorded				
Experimental testing	482	970	1456	1974
Numerical model	453	908	1360	1819
Difference	−6%	−6.4%	−6.6%	−7.9%
Maximum compressive strain ($x10^{-6}$) recorded				
Experimental testing	−474	−960	−1466	−1970
Numerical model	−453	−815	−1222	−1633
Difference (%)	−4.4%	−15.1%	−16.6%	−17.1%

holding for this length of time, only tests the actual set-up and not the blade itself and, therefore, holding the static load for 30 s yields the same information for the blade.

3.3. Fatigue testing

Fatigue testing was performed on the tidal turbine blade to determine if the blade could withstand the loadings imparted onto it for its 20-year design life. The fatigue testing of the blade was performed using a multi-actuator system to impart a hydraulic force/displacement excitation on the blade in line with the DNVGL-ST-0164 standard. An operational distributed load along the blade was determined from previous operational sea trials of Orbital Marine Power's SR-2000 turbine, where an equivalent distributed load was defined, with R = 0.1, that was suitable for use in laboratory conditions and would provide a continuous loading on the blade during the fatigue testing. The S–N curve, which defines the number of cycles to failure, N(S), when a material is repeatedly cycled through a given stress range S, for the composite material used to manufacture primary load bearing components (i.e. the spar caps), which is unidirectional glass fibre reinforced powder epoxy and given in (Finnegan et al., 2021b), is used to factor up the equivalent distributed load for the desired number of cycles for each phase of the fatigue testing programme. As discussed in Section 2.6.3, the fatigue testing programme was divided into two testing phases:

- Phase 1 used the equivalent distributed load accelerated for the laboratory testing and cycled for 200,000 cycles, which is the equivalent of 20-years operation at the actual operational load.
- Phase 2 used the equivalent distributed load that was factored by 1.39, to allow for factors of safety in line with the DNVGL-ST-0164 standard that accounts for differences between test and reality, and cycled for 100,000 cycles, which is the equivalent of 20-years operation at the factored operational load.

During the fatigue testing programme, the stiffness of the blade was monitored. This has been summarised by inspecting the hysteresis loops of moment imparted on the blade against tip deflection, which is presented in Fig. 11. During the Phase 1, there seems to be a slight change in blade stiffness, which is presented in Fig. 11 (a), but this may be, in part, due to the bedding-in of the test system during the initial stages of the test. For Phase 2, the load on the tidal turbine blade is increased, resulting in an increase in the blade deflection. However, very little change in blade stiffness is observed (Fig. 11 (b)).

Throughout the fatigue testing programme, the natural frequencies of the blade, which are presented in Table 1, were recorded to monitor any changes in the stiffness of the blade. An overview of the natural frequencies (in Hz) and standard deviations (SD) observed during the fatigue testing programme are presented in Table 3. During the fatigue testing, the stiffness of the blade in the flapwise direction was reduced slightly, which is evident from the reduction in the flapwise natural frequencies, but no other significant changes were observed. Three

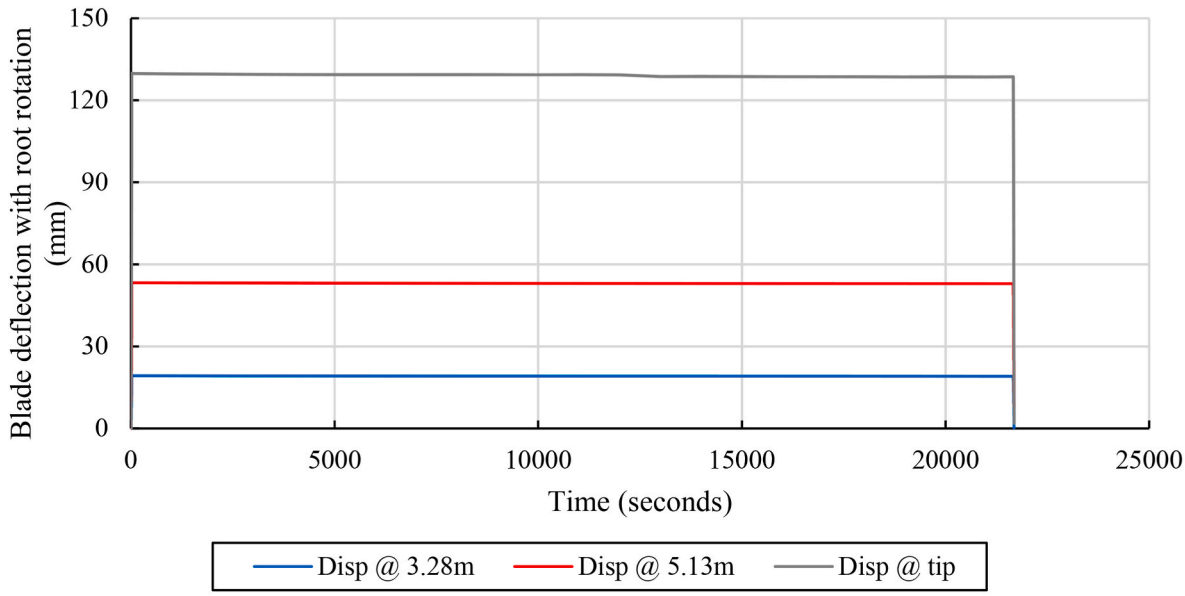

(a)

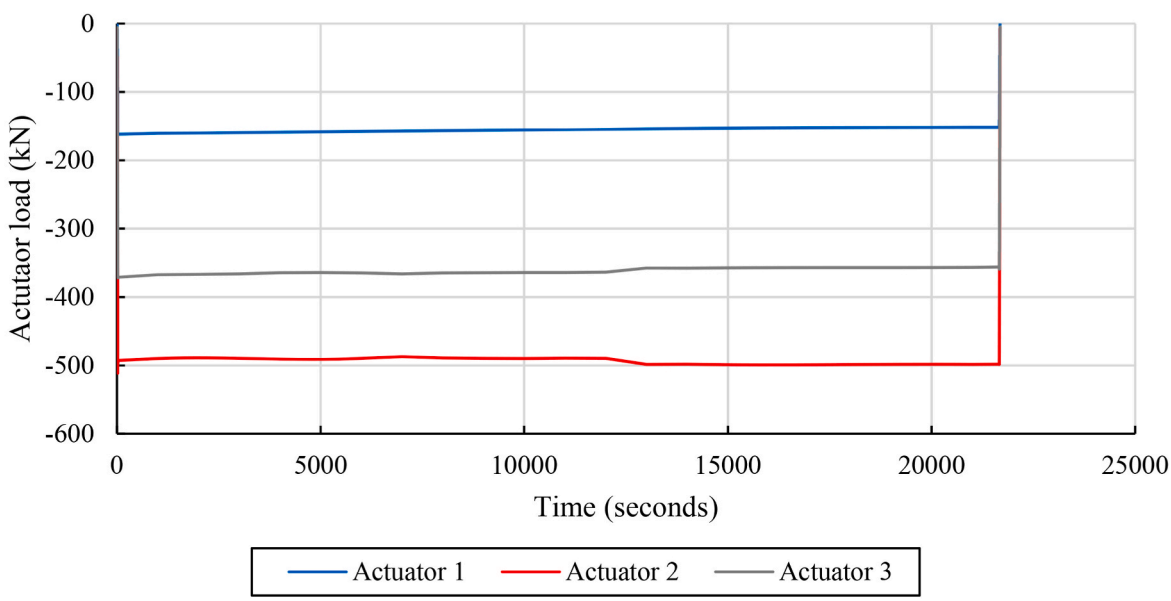

(b)

Fig. 10. Variation in the (a) blade deflection with root rotation due to flexing of the support frame and (b) imposed load over the 6-h static test at the 100% static load case.

dynamic tests were performed under each impact direction and the average results were used to estimate the natural frequencies, where the SD was also calculated and found to be low, between 0.003 and 0.085, showing confidence in the accuracy of the calculation method. Therefore, overall, there was no significant change in the blade stiffness during the fatigue testing, based on the results from the dynamic testing. This observation is consistent with the investigation of the moment-deflection response of the blade during testing.

3.4. Residual strength testing

After each phase of the fatigue testing programme, a residual strength test was performed in order to determine if any damage has occurred in the blade or if there has been a change in blade stiffness. For the residual strength testing, the maximum design static load was applied to the blade and compared across the three strength tests in order to estimate any drop-off in strength/stiffness of the blade. The load was applied through the 5 contact pads (with centres at 3.28m, 4.63m, 5.63m, 6.69m and 7.69m from the root) using the multi-actuator load introduction system. The load was held for a duration of 30 s before being removed and the loading were repeated at least 3 times to ensure repetition, where no significant difference between the loads applied (less than 1% change in overall load applied) were observed.

The resulting normalised deflection of the blade for each of the three strength tests is shown in Fig. 12 (a), where the tip deflection is 109 mm in each test, which does not take account of root rotation. It is evident

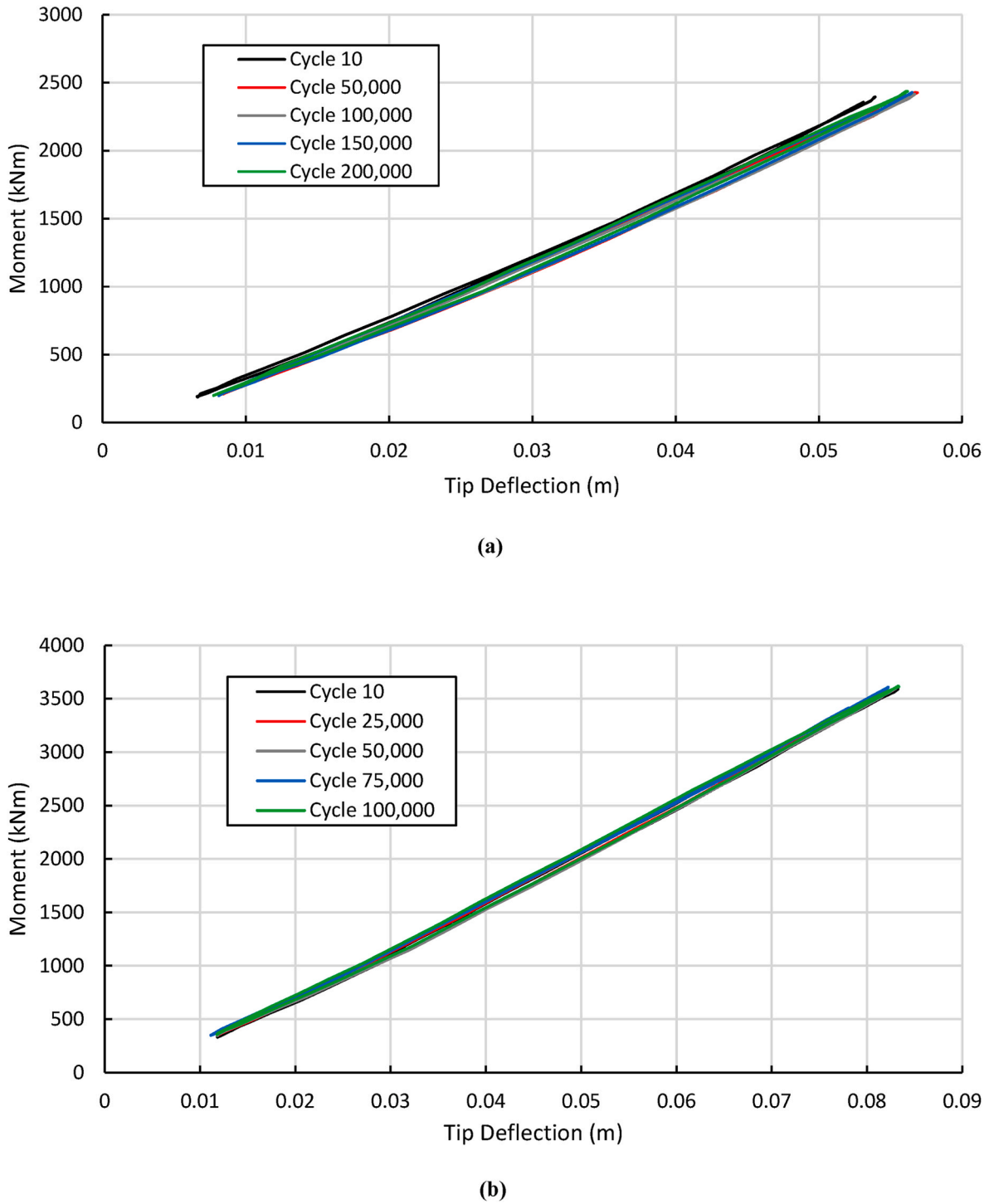

Fig. 11. Change in blade stiffness through monitoring the hysteresis loops of Moment against tip deflection for (a) the 200,000 cycles in Phase 1 and (b) the 100,000 cycles in Phase 2.

from Fig. 12 (a) that there was no significant difference (less than 2% change in any measurement) in the deflection of the blade when comparing the results during the two residual strength tests and the initial static test. Therefore, no significant drop-off in strength/stiffness of the blade has been observed during the fatigue testing. This finding is supported by the resulting normalised strains as no significant difference between the strains (less than ±3.5% change at any of the monitoring locations) during the three strength tests was observed. These normalised strains are presented in Fig. 12 (b) along the outer surface of the blade in the middle of the spar caps (on the pressure and suction side of the blade) for each of the three strength tests. Therefore, no significant drop-off in strength/stiffness of the blade has been observed during the fatigue testing. This is, again, consistent with the observation that there was very little change in the natural frequencies of the blade, shown in Table 3, meaning there was no significant change in blade stiffness as a result of the fatigue testing.

In addition, the blade substrate is glass fibre reinforced powder epoxy, where no failure in the material is expected until strains well in excess of ±0.0025 occur. Therefore, the blade design and manufacturing processes used are adequate to withstand the maximum design static

Table 3
Overview of the monitored natural frequencies (in Hz) and standard deviations (SD) of the blade throughout the fatigue testing programme.

	Natural frequency mode #									
	1st Flapwise		2nd Flapwise		1st Edgewise		2nd Edgewise		1st Torsional	
	Mean	SD	Mean	SD	Mean	SD	Mean	SD	Mean	SD
Initial	15.28	0.012	31.34	0.028	17.81	0.030	31.48	0.010	84.51	0.019
After 26k cycles	15.03	0.024	30.79	0.024	17.80	0.049	30.85	0.040	84.54	0.057
After 85k cycles	15.04	0.030	30.84	0.013	17.82	0.085	30.85	0.033	84.67	0.034
After 151k cycles	15.06	0.011	30.69	0.013	17.88	0.068	30.82	0.021	84.72	0.023
After phase 1	15.05	0.003	30.71	0.019	17.86	0.080	30.77	0.039	84.63	0.020
After 219k cycles	14.99	0.057	30.82	0.049	17.85	0.077	30.81	0.027	84.69	0.040
After 254k cycles	14.97	0.044	30.70	0.040	17.83	0.078	30.73	0.048	84.60	0.085
After 275k cycles	14.99	0.020	30.62	0.017	17.85	0.049	30.68	0.018	84.66	0.034
After phase 2	14.91	0.032	30.58	0.043	17.86	0.051	30.59	0.005	84.48	0.014

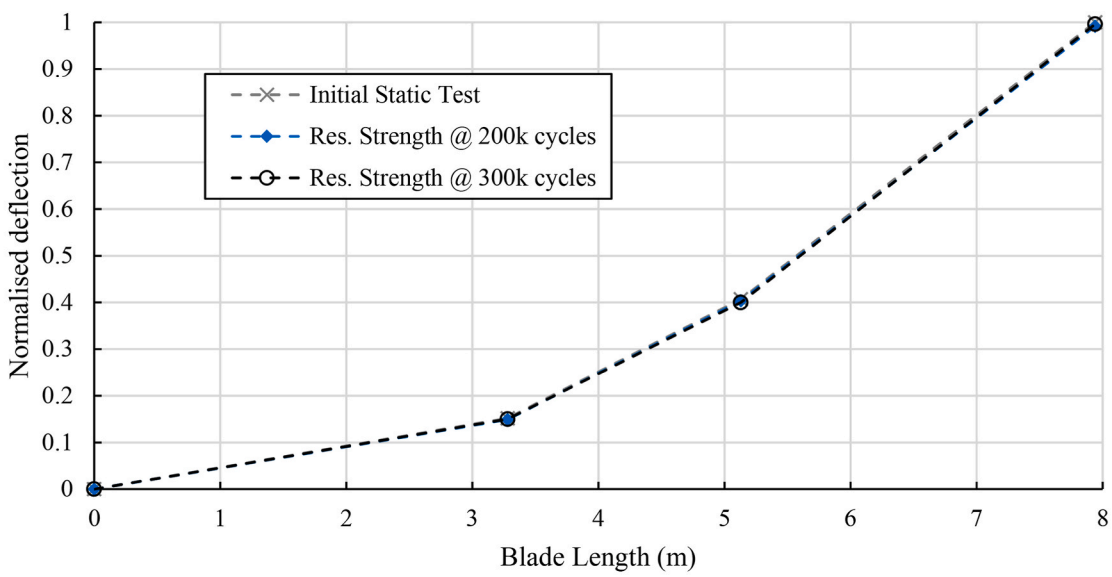

(a)

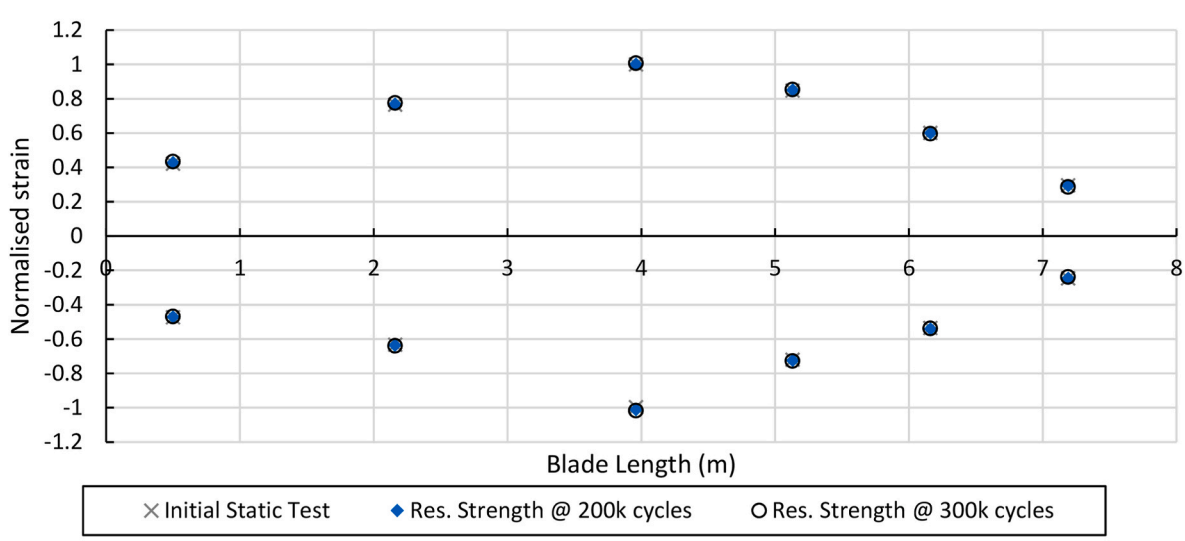

(b)

Fig. 12. Comparison between (a) the deflection (in mm) of the blade and (b) the strain ($x10^{-6}$) at the outer surface at the top and bottom spar caps along the length of the blade during the three strength tests.

loads.

4. Discussions

4.1. Numerical modelling

The digit twin of the composite structure of the tidal turbine blade is described in Section 2.4, where further details are available at (Jiang et al., 2021b). In order to ensure the comparison of the results from the testing campaign and the outputs from the numerical model are fair, the finite element model used in the blade design has been updated to include any changes to the design implemented during the blade manufacture. The outputs from this model have been compared to the results from the testing programme, which are found to be in very good agreement. Therefore, validating the accuracy of the model, where it now can be used to improve the efficiency of the blade, along with other tidal blades and composite components, during future design iterations.

4.2. Blade composite manufacture

The tidal turbine blade manufacture is described in Section 2.5, where further details are available at (Finnegan et al., 2021b). During the development of the blade manufacturing process, a number of innovations and technology developments were required, including thick section laminate manufacturing, blade roots connections and a one shot manufacturing process, which can withstand the high-loads and harsh marine environment during turbine operation. These technologies, which were enabled using an advanced glass fibre reinforced powder epoxy composite material, were validated by means of mechanical testing.

The thickness of the composite material along the spar caps and at the root of the blade is significantly thicker than that seen for most composites applications, where the composite was 130 mm in thickness at some locations. Therefore, it was necessary to design bespoke curing cycles, which included numerical modelling with experimental validation, and manufacturing trials along with edges of these thick sections, where it was found that the use of a caul plate with a height of the expected finish thickness of the section was the desired approach. For the current blade the root connection fixture also served as a caul plate to create a good quality root end. During manufacture, no issues with laminate thickness were observed.

The advanced root connection system using steel inserts, which was previously de-risked through mechanical testing, was installed during the layup of the composite material. It was observed that more time is required for the installation of these steel inserts during manufacture but this is offset, in part, by not needing to install a root connection system post cure, while providing a highly robust connection. It is noted that a further mechanical investigation of this system for a composite that has been submerged in water, similar to the operational environment, would yield more information about their performance during operation.

The composites manufacturing technologies used to produce the full-scale tidal turbine blades, which reduce the labour requirement during manufacture and ensure the blade survives the harsh operational environments over their design life, will help to move the tidal energy sector towards commercial viability. However, the introduction of automatic and additive manufacturing for the production of composites will need to be developed for volume production of these large composite structures.

4.3. Structural testing

This section discuss the outcomes and findings from the tidal turbine blade testing programme, which was performed in line with the IEC 62600–3:2020 test specification (International Electrotechnical Commission (IEC), 2020) and the DNV-ST-0164 tidal turbine testing standard (DNV, 2015). No damage was observed in the blade during either the static or fatigue testing programmes. However, some deviations from the IEC 62600–3:2020 test specification and the DNV-ST-0164 standard occurred during the testing, which are outlined in Table 4.

The successful completion of the static testing programme is a significant advancement for tidal energy as it saw the largest reported load ever applied to a tidal turbine blade in the world (at the 100% static test load of 1,008 kN). This helps to de-risk the technology as it proves the strength of the blade required to withstand very high loads in operation. In addition, the testing demonstrated that there is no need to hold a static load for more than 30 s, where the IEC 62600–3:2020 test specification recommends 6 h for tidal energy converters.

The completion of the fatigue testing has proven the 20-year design life of the blade, which is a world's first and a hugely important step forward in the certification of tidal turbine blades required for full commercialisation. The current guidelines for fatigue testing in the DNVGL-ST-0164 standard are based on the wind energy standards and there are limited guidelines in the IEC DTS 62600–3 testing specifications for fatigue testing. Therefore, the results of this study can help inform the next generation of fatigue test standards for tidal turbine blades. For example, as part of the design (Section 7.8.2.4) in the DNVGL-ST-0164 standard, it is advised that a conservative estimate for the maximum strain on glass-fibre reinforced epoxy laminates is a tensile strain of $\leq$0.35% and a compressive strain of $\leq$ |0.25%|. Based on the observations within this testing programme, these conservative limits are in good agreement with the values observed at the maximum design static loads on the blade.

Table 4
Conformance of the testing programme to the DNVGL-ST-0164 standard and the IEC 62600–3:2020 testing specifications.

Standard	Issue	Description
DNVGL-ST-0164 (18.2.5) IEC DTS 62600–3 (A.5.2)	Combined loading only used (primarily load in the flapwise direction)	Limitations on lab time due to complexity of installation and test set-up, only testing in one combined direction was performed. DNV GL standard allows for edgewise loading to be omitted if not critical, which is the case here. IEC test specification specifies testing the static blade root edgewise bending moment as "Recommended".
DNVGL-ST-0164 (18.2.6)	Application of dead weights to achieve the correct load distribution	As a multi-actuator system is used to impart the hydraulic load on the blade that uses 3 actuators, it was possible to apply the load through contact pads at 5 points. Therefore, the correct load distribution could be achieved with the multi-actuator system alone.
DNVGL-ST-0164 (18.2.7)	It is recommended, that after successfully performing the fatigue testing as per [18.2.6], a residual strength test is performed.	Since the fatigue testing was divided into 2 phases, a residual strength test was performed after each phase.
IEC DTS 62600–3 (A.8.3)	Static testing was held for 30 s before relaxing	DNV state a minimum duration of 10 s and the IEC a minimum duration of 30 s. However, the IEC also states "for TECs the recommended minimum duration of the test load is 6 h". The design loads have short durations so 30 s is acceptable. A 6-h test was performed (detailed in Section 3.2.2) and found that no significant changes occur over this duration.

5. Conclusion

This paper presents the development of a full-scale fibre-reinforced composite blade for use on 1 MW power generating nacelles of a tidal turbine from design to structural testing. The digital twin in the form of a numerical finite element model that is used in its design has been detailed and validated using the results from the structural testing. Due to the high loads and harsh environment that a tidal turbine operates in, advanced manufacturing technologies have been developed to produce (i) thick section composites in excess of 130 mm for the key structural elements (i.e. the spar caps and at the root), (ii) a novel high-friction root connection, and (iii) cured bonds along the leading and trailing edge that are more robust than using adhesives. The full-scale tidal turbine blade then underwent an advanced structural testing programme that proves its structural integrity, where it is the largest blade to undergo a full lifetime fatigue programme (equivalent of 20+ years) and has the highest mechanical load ever reported on a tidal turbine blade. The results provide the first full-scale testing of the one-shot process using powder epoxy on thick composite sections and, also, demonstrates that the technology is very well suited to tidal blade manufacture. The structural testing programme also highlighted a number of best practices that could be introduced to the next revision of both the IEC 62600–3:2020 test specification and the DNV-ST-0164 standard: using a combined flapwise-edgewise loading as it is replicative of the operational conditions of the blade and reduces resource requirements of the test; the use of a multi-actuator load introduction system to ensure the correct load distribution can be achieved; and, during static testing, holding the load for 30 s at each load case is sufficient, as no significant change in the blade is seen thereafter.

The technologies developed in this paper, relating to design, manufacturing and testing, will, not only, benefit the tidal turbine developer and blade manufacturer, but will also the tidal energy sector as a whole, as it increases the reliability and robustness of the blades. Ultimately, the results of this study will aid in lowering the levelised cost of tidal energy and increase the design life of tidal turbine blades to over 20 years by ensuring that tidal turbine blades have the best chance of surviving the harsh environment in which they are deployed. The longevity of the blades and their ability to withstand high mechanical loadings, both static and fatigue, throughout their design life span will significantly reduce maintenance costs and allow for uninterrupted energy generation, therefore decreasing the levelised cost of tidal energy.

CRediT authorship contribution statement

William Finnegan: Conceptualization, Data curation, Formal analysis, Funding acquisition, Investigation, Methodology, Project administration, Writing – original draft. **Yadong Jiang:** Data curation, Investigation, Formal analysis, Writing – original draft. **Patrick Meier:** Investigation. **Le Chi Hung:** Investigation. **Edward Fagan:** Investigation, Methodology. **Finlay Wallace:** Formal analysis, Investigation, Methodology. **Michael Flanagan:** Investigation, Supervision. **Tomas Flanagan:** Funding acquisition, Investigation, Methodology, Project administration, Supervision. **Jamie Goggins:** Funding acquisition, Investigation, Methodology, Writing – original draft, Project administration, Supervision.

Declaration of competing interest

The authors declare that they have no known competing financial interests or personal relationships that could have appeared to influence the work reported in this paper.

Data availability

Data will be made available on request.

Acknowledgments

This research was funded by European Commission, through the H2020 MaRINET2 project (grant agreement no.: 26255), H2020 FLOTEC (grant agreement no.: 691916) and the H2020 CRIMSON project (grant agreement no.: 971209), and the Sustainable Energy Authority of Ireland (SEAI), through the Ocean ERA-NET Ocean Energy Prototype Research and Development Programme 2018 as part of the SEABLADE project (Award no.: 18/OCN/102). The first, second and last authors would like to acknowledge the support from Science Foundation Ireland (SFI), through the MaREI Research Centre for Energy, Climate and Marine (Grant no. 12/RC/2302_2).

References

ANSYS, 2016. Ansys Academic Research Mechanical, Release 17.1: Mechanical Application Documentation. ANSYS Inc., Pennsylvania, United States.
ANSYS, 2017. ANSYS® CFX (Release 17.1): CFX-Solver Theory Guide. ANSYS Inc.
Brádaigh CMÓ, Doyle A, Doyle D, Feerick PJ. One-shot wind turbine blade manufacturing using powder-epoxy and electrically-heated ceramic composite tooling. 7th International CFK-Valley Stade Convention. Germany2013.
Chopra, A.K., 2007. Dynamics of Structures, third ed. Prentice Hall, New Jersey.
Collombet, R., 2021. Ocean Energy: Key Trends and Statistics 2020. Ocean energy Europe (OEE), Brussels, Belgium.
de la Torre, O., Moore, D., Gavigan, D., Goggins, J., 2018. Accelerated life testing study of a novel tidal turbine blade attachment. Int. J. Fatig. 114, 226–237.
Dnv, G.L., 2015. Tidal Turbines. DNV Standard, DNVGL-ST-0164. Oslo, Norway.
EC, 2020. An EU Strategy to Harness the Potential of Offshore Renewable Energy for a Climate Neutral Future. European Commission, Brussels, Belgium.
Fagan, E.M., Kennedy, C.R., Leen, S.B., Goggins, J., 2016. Damage mechanics based design methodology for tidal current turbine composite blades. Renew. Energy 97, 358–372.
Finnegan, W., Fagan, E., Flanagan, T., Doyle, A., Goggins, J., 2020. Operational fatigue loading on tidal turbine blades using computational fluid dynamics. Renew. Energy 152, 430–440.
Finnegan, W., Jiang, Y., Dumergue, N., Davies, P., Goggins, J., 2021a. Investigation and validation of numerical models for composite wind turbine blades. J. Mar. Sci. Eng. 9 (5), 525.
Finnegan, W., Allen, R., Glennon, C., Maguire, J., Flanagan, M., Flanagan, T., 2021b. Manufacture of high performance tidal turbine blades using advanced composite manufacturing technologies. Appl. Compos. Mater. 314.
Flanagan T, Maguire J, Brádaigh CMÓ, Mayorga P, Doyle A. Smart Affordable Composite Blades for Tidal Energy. European Wave and Tidal Energy Conference (EWTEC 2015). Nantes, France2015.
Garanovic, A., 2020. RivGen Sets US Marine Hydrokinetic Turbine Record. Offshore Energy, The Netherlands. URL: https://www.offshore-energy.biz/rivgen-sets-us-marine-hydrokinetic-turbine-record/. (Accessed 12 April 2022).
Glennon, C., Finnegan, W., Kaufmann, N., Meier, P., Jiang, Y., R, S., et al., 2021. Tidal stream to mainstream: mechanical testing of composite tidal stream blades to de-risk operational design life. J. Ocean Eng. Mar. Energy.
Grogan, D., Flanagan, M., Walls, M., Leen, S., Doyle, A., Harrison, N., et al., 2018. Influence of microstructural defects and hydrostatic pressure on water absorption in composite materials for tidal energy. J. Compos. Mater. 52 (21), 2899–2917.
Gurit, 2016. Exothermic Reactions. Gurit.
International Electrotechnical Commission (IEC), 2020. IEC TS 62600-3:2020 Marine Energy - Wave, Tidal and Other Water Current Converters. Part 3: Measurement of Mechanical Loads. IEC, Geneva, Switzerland.
Jiang Y, Fagan E, Goggins J. Structural Design and Optimisation of a Full-Scale Tidal Turbine Blade. 13th European Wave and Tidal Energy Conference (EWTEC) Naples, Italy2019.
Jiang, Y., Fagan, E., Goggins, J., 2021a. BladeComp – a Design and Optimisation Software for Wind and Tidal Turbine Blades. National University of Ireland Galway, Galway, Ireland.
Jiang, Y., Finnegan, W., Wallace, F., Flanagan, M., Flanagan, T., Goggins, J., 2021b. Structural analysis of a 1 MW tidal turbine blade through full-scale physical testing and a digital twin. Marine. In: 9th Conference on Computational Methods in Marine Engineering. https://doi.org/10.2218/marine2021.6799.
Maguire, J.M., Sharp, N.D., Pipes, R.B., Brádaigh, C.M.Ó., 2017. Process Simulations for Manufacturing Thick-Section Parts with Low-Cost Fibre Reinforced Polymers. SAMPE Europe Conference, Stuttgart, Germany2017.
Maguire, J.M., Nayak, K., Ó Brádaigh, C.M., 2018. Characterisation of epoxy powders for processing thick-section composite structures. Mater. Des. 139, 112–121.
Maguire, J.M., Simacek, P., Advani, S.G., Ó Brádaigh, C.M., 2020. Novel epoxy powder for manufacturing thick-section composite parts under vacuum-bag-only conditions. Part I: through-thickness process modelling. Compos. Appl. Sci. Manuf. 136, 105969.
Matveev, M.Y., Belnoue, J.P.H., Nixon-Pearson, O.J., Ivanov, D.S., Long, A.C., Hallett, S. R., et al., 2019. A numerical study of variability in the manufacturing process of thick composite parts. Compos. Struct. 208, 23–32.
Meier P, Finnegan W, Cronin P, Donegan J, Barrington M, Le Hung C, et al. Static and Fatigue Testing of A Full Scale Helical River Turbine Foil. Civil Engineering Research in Ireland 2020. Cork, Ireland2020.

Michael, W., Heather, O.C., P, D.D., Jamie, G., 2019. Testing of hydrophobically coated composite materials with marine energy applications. Infrastr. Asset Manag. 1–11, 0 (0.

Murray, R.E., Nevalainen, T., Gracie-Orr, K., Doman, D.A., Pegg, M.J., Johnstone, C.M., 2016. Passively adaptive tidal turbine blades: design tool development and initial verification. Int. J. Mar. Energy 14, 101–124.

Orbital Marine Power. Latest News. URL: https://orbitalmarine.com/news/. (Accessed 12 April 2022).

SIMEC Atlantis Energy. SAE achieves another tidal milestone in Japan. URL: https://simecatlantis.com/2021/05/24/sae-achieves-another-tidal-milestone-in-japan/. (Accessed 12 April 2022).

SIMEC Atlantis Energy. Tidal energy projects: meygen. United kingdom: SIMEC Atlantis energy. URL: https://simecatlantis.com/projects/meygen/. (Accessed 12 April 2022).

Vaidya, U.K., Young, W., Ulven, C., 2001. Affordable Processing of Thick Section Composite Structures. 11th International Offshore and Polar Engineering Conference. Stavanger, Norway. The International Society of Offshore and Polar Engineers.

Voc, E.C., 1999. Solvent Emissions Directive 1999/13/EC. Council of the European Union, Brussels, Ireland.